Tailoring the dynamics of diode lasers by passive dispersive reflectors

Uwe Bandelow[a], Mindaugas Radziunas[a,c], Vasile Tronciu[b],
Hans-Jürgen Wünsche[c], and Fritz Henneberger[c]

[a] Weierstraß-Insitut für Angewandte Analysis und Stochastik, Mohrenstr. 39, D-10117 Berlin, Germany.

[b] Technical University of Moldova, Department of Physics, Stefan cel Mare 168, Chisinau MD-2004 Moldova

[c] Humboldt-Universität zu Berlin, Institut für Physik, Invalidenstr. 110, D-10115 Berlin, Germany.

ABSTRACT

Possibilities are investigated for influencing the dynamical behaviour of diode lasers by means of integrated passive dispersive reflectors (PDR). The specific configurations comprise DFB lasers complemented with different PDR, which consist of a phase tuning section and a passive grating section. Among others, the potential of these configurations will be investigated for generation and tuning the properties of self pulsations (SP), as e.g. the frequency and the modulation depth. Our considerations are based on the Traveling Wave Equations (TWE) coupled to carrier rate Equations. Together with numerical time domain computations of this system, a single mode approximation is applied and checked as possible tool for tailoring the dynamic effects.

Keywords: laser, dynamics, dispersion, traveling wave equations, modes

1. INTRODUCTION

It is well known that optical feedback can considerably influence the dynamical behaviour of a semiconductor laser. Already simple reflections at distant external mirrors like fiber connectors can cause interesting phenomena as, e.g., coherence collaps, low frequency fluctuations, or self-pulsations (SP). These effects have been investigated intensively since many years (see, e.g.,[1–3] and references therein).

In this paper, we consider a special situation where the feedback comes from a dispersive reflector (a Bragg grating) that is integrated together with the laser within a compound and compact device as sketched in Fig. 1.

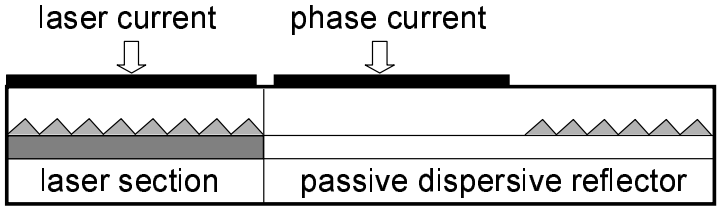

Figure 1. *Basic device structure. A DFB laser is connected with a passive dispersive reflector (PDR) containing a tunable phase shift section and a passive grating section.*

Similar devices[4] are used to generate high-frequency self-pulsations (SP) and serve very successfully as optical clock in the data regeneration.[5] Those devices use identical transverse structures for both DFB sections. But only the laser section is highly pumped and produces gain. In contrast, the DFB-reflector is driven close to the transparency current.[4,6] The carrier-light coupling is small in this regime and the section acts nearly as a passive reflector. In the present paper, we draw the consequence and assume a completely passive DFB reflector. This design could be realized, e.g., by using the same waveguide structure as in the phase tuning part. Here, the active 1.55μm layer is replaced by an layer at 1.3μm not coupling to the laser light. The carriers generated in this layer by the phase tuning current do not produce gain but mainly change the phase shift via the effective refractive index of the waveguide. When using this design also in the DFB reflector part, no pump current has to be considered as sketched in Fig. 1, which is our convention in the following. However, a pump current could possibly be useful to tune the

Further author information: Send correspondence to U.B., http://www.wias-berlin.de, E-mail: bandelow@wias-berlin.de

spectral position of the stop band of the reflector. One question to be investigated theoretically in this paper is, whether fast SP can also be generated with such completely passive dispersive reflectors (PDR). Furthermore, we try to find out how much the properties of the SP can be tailored by appropriately designing the reflector.

The basic model equations will be presented in the next chapter. An analysis of the impact of a PDR on the nonlinear dynamics by means of single mode equations follows. An increase of the resonance frequency of the laser and a modification of its damping are obtained. Conditions for achieving either fast swiching between stationary states or fast and well modulated SP will be derived. This single mode analysis is confirmed and deepened in chapter 4 by results of time domain simulations taking into account all relevant modes. Some tendency to undesirable mode hopping is found as a new effect not visible in the single mode analysis. On this base, it is shown in section 4.2 that the detuning between the gratings of the laser and reflector sections can be used as a design parameter for suppressing the mode hopping.

2. TRAVELING WAVE EQUATION MODEL

The optical field inside laser is decomposed into forward and backward propagating waves with corresponding slowly varying amplitudes $\Psi^+(z,t)$ and $\Psi^-(z,t)$, which obey the well known Traveling Wave Equations (TWE)[7]:

$$\begin{aligned} \left(-iv_g^{-1}\partial_t - i\partial_z + \beta\right)\Psi^+ + \kappa_+\Psi^- &= 0 \\ \left(-iv_g^{-1}\partial_t + i\partial_z + \beta\right)\Psi^- + \kappa_-\Psi^+ &= 0. \end{aligned} \tag{1}$$

The partial derivatives with respect to the time t and the longitudinal position z are denoted by ∂_t and ∂_z, respectively. Spontaneuos emission is neglected here, because the phenomena of interest appear well above threshold. The group velocity v_g, and the coupling coefficients κ_+ and κ_- of the Bragg gratings are constant within each section. For the index grating parts of our device it holds $\kappa_- = \kappa_+^*$. The end facets ($z = 0$ and $z = L$) are AR-coated and we have no external injection of light, thats why the field amplitudes obey the boundary conditions $\Psi^+(0,t) = 0$ and $\Psi^-(L,t) = 0$. The relative wave number β is differently modeled in the different parts of the device.

In the grating part of the PDR, the constant value $\beta = -i\alpha_r/2$ is used with the optical losses α_r. This implies that the center of the stopband of the reflector grating is taken as the central wavelength. In the phase tuning part of the PDR which has the length l_p, we use $\beta = \delta_p - i\alpha_p/2$. In general, the detuning parameter δ_p as well as the losses α_p would depend on the injected current. For modelling purposes it is however more appropriate to use the phase shift $\varphi = \delta_p l_p/\pi$ as a control parameter.

In the laser section we have to take into account an electronic contribution to β due to the gain and the influence of the carrier density N on the refrective index, as well as a possible static detuning δ relative to the reflector grating,

$$\beta = \delta - i\frac{\alpha_0}{2} + \frac{1}{2}(\alpha_H + i)\Gamma g'\left[N - N_{tr}\right] \qquad \text{(in laser section)} \tag{2}$$

The parameters $\alpha_0, \alpha_H, \Gamma, g'$, and N_{tr}, represent the internal optical losses, Henry's linewidth enhancement factor, the transverse modal fill factor, the differential gain, and the transparency concentration, respectively, of the corresponding section. Excluding effects of spatial hole burning, the spatially constant carrier density is governed by the balance equation

$$\frac{d}{dt}N = \frac{I}{eV} - R(N) - v_g\Gamma g'\left[N - N_{tr}\right]S, \tag{3}$$

where

$$S = \frac{1}{V}\int_{laser} |\Psi^+(z,t)|^2 + |\Psi^-(z,t)|^2 \, dz \tag{4}$$

is the photon density averaged over the volume V of the active zone, e is the electron charge and I represents the total current injected into the laser section. All spontaneous channels are summarized in the second term, which is parametrized as usual in the polynomial form $R(N) = AN + BN^2 + CN^3$.

3. SINGLE MODE DYNAMICS

In many cases, the dynamics of a laser is governed by only one dominant mode. Then the TWE (1) can be replaced by a photon rate equation that has been derived in.[8] This approximation has been very successfully applied to devices with an active DFB reflector.[9] In this chapter, we use it to find possibilities for modifying the dynamics of a laser by passive dispersive reflectors.

3.1. Dimensionless rate equations

The following dimensionless normal form of these equations is used:

$$\frac{dn}{d\tau} = J - n - (1+n)K(n)p \qquad \frac{dp}{d\tau} = T\,G(n)\,p. \tag{5}$$

The dimensionless time variable τ and the carrier life time T are measured in units of the photon life time, hence, T is typically in the order of 10^3. J and n are dimensionless representatives for the pump current and the carrier density in the laser section, with $J = 0$ and $n = 0$ at the threshold, respectively. p is a normalized photon number. More details and a derivation of these equations as well as a proof of the following statements will be given elsewhere.[10]

Without a reflector, i.e., for a solitary DFB laser, one finds always $K(n) \equiv 1$ and $G(n) = n$. This means

i) that any single section DFB laser is described by reduced rate equations with only two parameters, J and T, and,

ii) that the qualitative influence of a dispersive reflector can come into the play only via the two functions $K(n)$ and $G(n)$.

Thus, the task is to investigate the dynamics of Eqs. (5) in dependence on these two functions.

To solve this task, we have looked for the typical shape of $K(n)$ and $G(n)$. Some examples can be found in the literature. Single section DFB-reflectors with a uniform index coupled grating were investigated in.[11,7] A narrow resonance-like enhancement was found as most prominent feature for the axial factor K_z of excess spontaneous emission, which is the main constituent of $K(n)$. This behaviour could be attributed to a nearby point of mode degeneracy at which K_z diverges.[7] Similar results were obtained in[9] for more complicated reflectors composed of a DFB section accomplished by a phase tuning section. We believe that such resonances of K_z due to degeneracy points are a rather general consequence of dispersive reflectors. Using the formulae of Ref.[9] , we have calculated $K(n)$ for different reflector structures and found always such a resonance. One typical example is drawn in Fig. 2 (solid line).

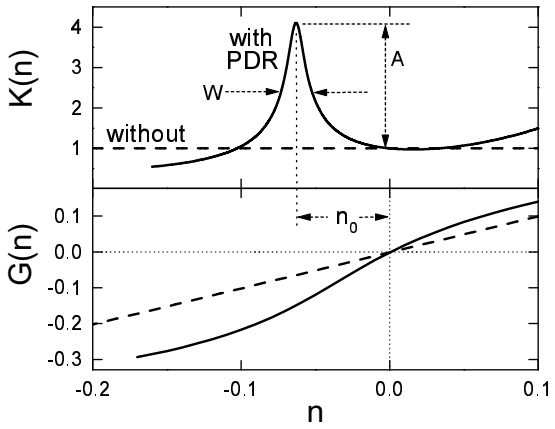

Figure 2. *The RE functions $K(n)$ and $G(n)$. Dashed: Solitary DFB-laser. Solid: Numerical calculation for a typical DFB laser with dispersive reflector.*

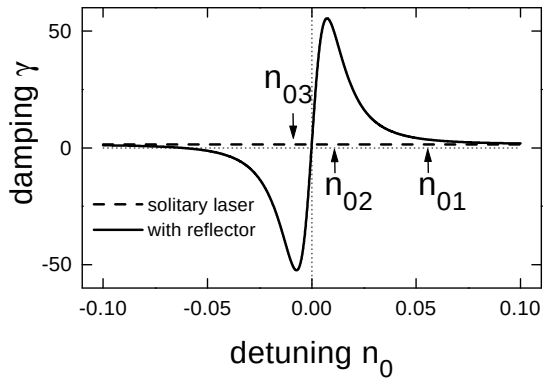

Figure 3. *Dependence of the damping γ on the detuning n_0 for $J = 2$. Dashed: solitary laser. Solid: laser with a dispersive reflector ($W = 0.02, A = 1$).*

The position n_0 of the resonance, its width W and height A vary in wide limits depending on the parameters of the reflector. To study the consequences of these different configurations on the dynamics, we use the simple Lorentzian model

$$K(n) = K_0 + \frac{A\,W^2}{4(n-n_0)^2 + W^2} \tag{6}$$

and vary n_0, W, and A. The parameter K_0 is not free, but fixed by the normalization condition $K(0) = 1$.

The lower part of Fig. 2 gives a typical example for the influence of dispersive reflectors on $G(n)$. It is mainly an enhancement of its slope within a finite density interval. This feature is also modeled by a simple function,

$$G(n) = n + \alpha\,\Delta\,\tanh\left(\frac{n}{\Delta}\right). \tag{7}$$

Here, the maximum slope is $1+\alpha$ and the width of the slope enhancement region is characterized by Δ.

3.2. Stability of the Equilibria

Above threshold ($J > 0$), the on-state of the laser is given by the stationary solution $(n_1, p_1) = (0, J)$ of Eqs. (5). To determine the stability of this solution we compute the eigenvalues of the Jacobian of the right-hand side of (5) at this point. We find the pair of complex eigenvalues

$$\lambda_\pm = -\gamma \pm i\sqrt{\omega^2 - \gamma^2} \qquad \text{with} \quad \gamma = \frac{1}{2}\left[1 + (1 + K'(0))\,J\right], \quad \omega^2 = T\,G'(0)\,J. \tag{8}$$

In case of a solitary laser described by $K(n) \equiv 1$ and $G(n) \equiv n$, the on-state (n_1, p_1) is a stable focus with damping $\gamma = (1+J)/2$ and frequency $\omega = \sqrt{TJ}$ provided $\omega^2 > \gamma^2$. The expressions in (8) show the different influences of the values $K'(0)$ and $G'(0)$. The resonance frequency ω of the laser becomes modified only by $G'(0) = 1 + \alpha$, i. e., by the slope enhancement due to the presence of the dispersive reflector. This effect has already been demonstrated and exploited by Kjebon et al.[12] to achieve very large modulation band widths up to 30 GHz. The damping γ, on the other hand, that is responsible for the stability, is influenced by $K'(0)$ only.

Now we study how the stability of the on-state depends on the parameters A and n_0 for fixed W. A simple analysis shows that the damping γ as a function of n_0 has at most two roots for any A and W. If A is sufficiently large, the function $\gamma(n_0)$ has two simple zeroes, its graph is shown in Fig. 3 (solid line). This curve visualizes that the resonance of $K(n)$ affects the stability of the on-state only if its position is within an interval near threshold. In this region the damping is strongly enhanced for $n_0 > 0$. For large A and decreasing n_0 the stability of the on-state changes rapidly near $n_0 = 0$ from a strongly damped focus to a strongly unstable focus. For $|n_0| \gg W$ the resonance of $K(n)$ does not influence the damping of the on-state. It is as small as without PDR (dashed line in Fig. 3). We conclude that the introduction of a PDR changes essentially the behaviour of damping.

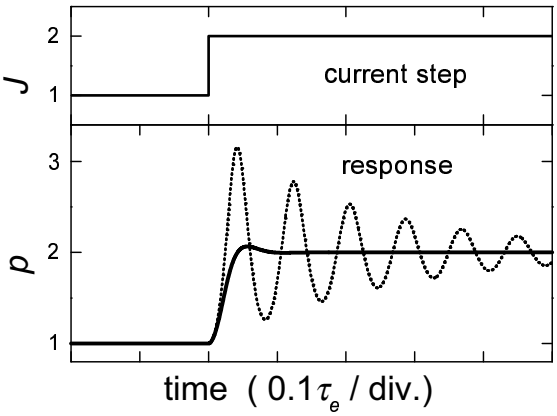

Figure 4. *Influence of a reflector on the response of the reduced photon number p to a current step. Dashed: normal damping ($n_0 = n_{01} = 0.05$). Solid: enhanced damping ($n_0 = n_{02} = 0.005$). Parameters as in Fig. 5.*

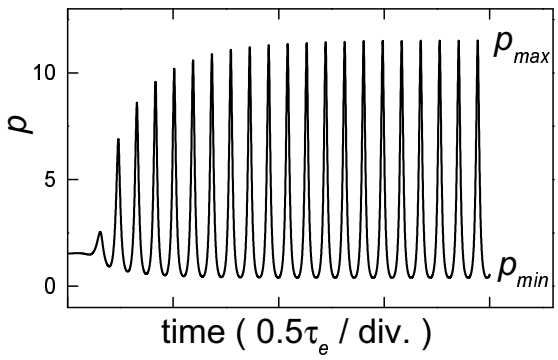

Figure 5. *A developing self-pulsation of the reduced photon number for the detuning $n_0 = n_{03} = -0.005$ (negative damping). Further parameters: $J = 2$, $W = 0.02$, $A = 1$, $\alpha = 5$, $\Delta = 0.1$.*

Now we demonstrate how the region of enhanced positive damping can be used to modify the switching between stable steady states. For this purpose we apply a current step and compare the time behaviour of the reduced photon number p for two different values of detuning (Fig. 4). The first one $n_0 = n_{01} = 0.05$ (dashed) corresponds to the damping of a solitary laser (cf. Fig. 3). The most important feature of the transient response is here that the switching is accompanied by weakly damped relaxation oscillations. The second detuning $n_0 = n_{02} = 0.005$

corresponds to the enhanced damping in Fig. 3. In this case, the transient response (full line) practically reflects the form of the injected current such that the switching time is very much shorter compared with the solitary laser. For the negative detuning $n_0 = n_{03}$, the stationary state corresponding to J=2 is unstable (cf. Fig. 3). Starting from this state, numerical noise causes a transition into a self-pulsation (Fig. 5), even when keeping J constant. These self-pulsations will be discussed in more detail in the following subsection.

3.3. Bifurcation Analysis

In the previous subsection we have shown that the stationary lasing state is unstable for sufficiently large amplitude A if the detuning n_0 belongs to some interval $B_2 < n_0 < B_1 < 0$. Since $\gamma(n_0)$ has simple zeroes for $n_0 = B_2$ and $n_0 = B_1$, these points are Hopf bifurcation points. In this subsection we explore the families of periodic solutions we expect to emerge at the Hopf points B_1 and B_2 and compute the bifurcation curves in the (A, n_0)-plane *.

Varying both parameters n_0 and A we obtain the Hopf curve P_1-P_2-P_3 in the (A, n_0)-plane where the curve P_1-P_2 is a supercritical Hopf curve and the curve P_2-P_3 is a subcritical Hopf curve. At the point P_2 the Hopf bifurcation is degenerated and a branch of saddle-node bifurcations of periodic solutions emerges (the curve P_2-P_4 in Fig. 6). These bifurcation curves divide the parameter plane into three regions. The on-state is the only attractor in region I. It is unstable and the SP is stable in region III. In region II the stable stationary lasing state and a stable SP coexist and are separated by an unstable periodic solution. Which of the two stable solutions hold depends on the history of the device, i.e., hysteresis appears in this region. Coming from region I, the system stays in the stationary stationary lasing state, whereas it stays in the SP state when coming from region III.

The other parameters influence the bifurcation curves of Fig. 6 in the following manner: a decrease of W contracts the regions II and III where P_3 and P_4 are shifted towards P_1. At the same time the minimum of the Hopf curve tends to the origin. A change of α or Δ implies only a minor change of the line P_2-P_4 and has no influence on the line $P_1 - P_2 - P_3$.

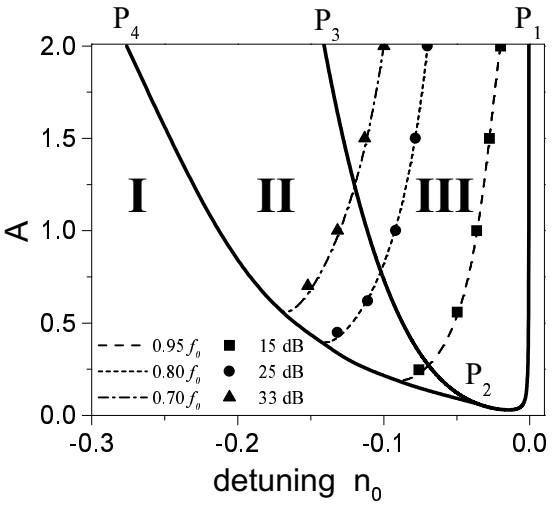

Figure 6. *Thick lines: Decomposition of the (n_0, A)-plane in three regions with different qualitative behaviour. Thin lines: Isofrequency contours, i.e., curves with the same frequency of self-pulsations. Big marks: loci of a given modulation depth measured in terms of dB= $10\lg(p_{\max}/p_{\min})$. Parameters: $W = 0.05, \mathcal{J} = 2$ and $\alpha = 0$.*

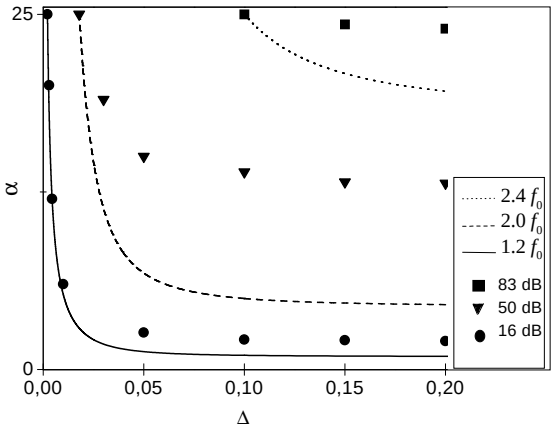

Figure 7. *Contours of constant frequency and modulation depth in the (α, Δ)-plane for parameters $W = 0.02, \mathcal{J} = 2$ and $A = 0.5, n_0 = -0.025$.*

Now we are interested in tuning (in the sense of increasing) the frequency f of the stable self-pulsations compared with the relaxation frequency $f_0 = \sqrt{T\mathcal{J}}/2\pi$ of the solitary laser. Without an enhanced gain slope ($\alpha = 0$), our numerical investigations yield for any W the following results (see Fig. 6). It is $f = f_0$ just on the curve $P_1 - P_2$ of supercritical Hopf bifurcation, where the modulation depth $m = P_{max}/P_{min}$ of the SP vanishes. With increasing

*The bifurcation detection and continuation software package AUTO has been used to perform the numeric computations.[13]

distance from this curve, each curve of constant f is still very close to a curve of constant m. With increasing modulation depth m the frequency f decreases.

Next we fix a point in region III and draw the curves of the constant frequency and the curves of the same modulation depth in the (α, Δ)-plane (Fig. 7). This picture shows that the frequency and the modulation depth increase with increasing α if Δ is sufficiently large, i. e. the interval of gain enhancement covers the variation of n along the orbit of the SP. Furthermore, the frequency of the SP is larger than f_0 for $\alpha > 0$. At the same time, high modulation depths can be achieved if α and Δ are sufficiently high.

Summarizing this chapter, we draw the following conclusions: A PDR influences the dynamics of a single-mode laser by a narrow resonance-like enhancement of the function K and a local gain enhancement. The amplitude and the position of the resonance of the function K control the existence of self-pulsations and the stability of the stationary lasing state. There are parameter constellations where the PDR laser can be used for fast optical switching. An increase of the frequency of the SP beyond the relaxation frequency of a single section device can not be obtained by means of the parameters of the function K, however an increasing of the slope of the local gain enhancement allows to reach this goal.

4. MULTI MODE TIME DOMAIN SIMULATIONS

In this section we check the single mode analysis of the previous chapter by the more complicated numerical simulation based on the full equations given in section 2. Details of the numerical model and its confirmation by comparison with measurements will be given elsewhere.[14] Here we focus on the demonstration that single mode SP can also be generated by completely passive dispersive reflectors. From previous experimental and theoretical work on devices with active DFB reflectors we know the following specific criteria for generating single mode SP by Dispersive self Q-Switching (DQS):

a) the lasing mode is positioned on the negative slope of the reflectors reflectivity spectrum,

b) the SP are turned on by adjusting appropriate phase conditions.

Using the same set of device parameters as in[14] but keeping the reflector grating passive, we indeed obtain SP of the desired type when choosing the spectral situation depicted in Fig. 8 and an appropriate phase condition. In a next step we use the phase condition for controling the SP.

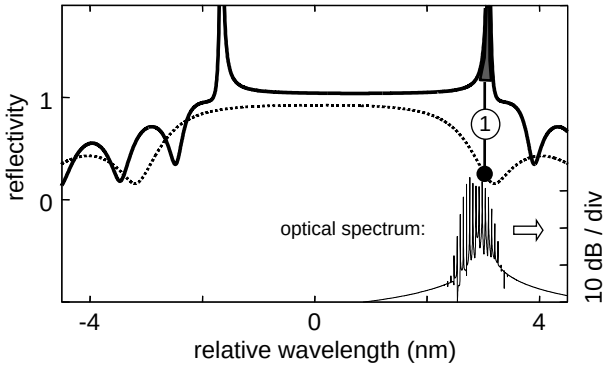

Figure 8. *Feedback spectra of the gain section (thick solid) and of the reflector section (thick dotted), calculated for one moment during the SP. Thin solid: Optical spectrum of a corresponding SP, calculated from the output at the facet of the laser section.*

4.1. Controling the dynamics by phase tuning

The phase of the light fed back from the reflector into the laser can easily be varied by changing the phase tuning current. It is therefore an important parameter for controling the dynamics induced by the dispersive reflector. In this subsection, we vary this parameter and keep all other parameters fixed.

The main results of the time domain simulations are collected in Fig. 9 as thick full and dashed lines. Part a) shows either the stationary output after the decay of the relaxation oscillations or the maximum and the minimum power during one period of a self-pulsation. The vertical lines labeled by capitals mark some points for the discussion. In all cases except at point B, the lasing emission is carried by one distinguished dominant mode. The + or - sign

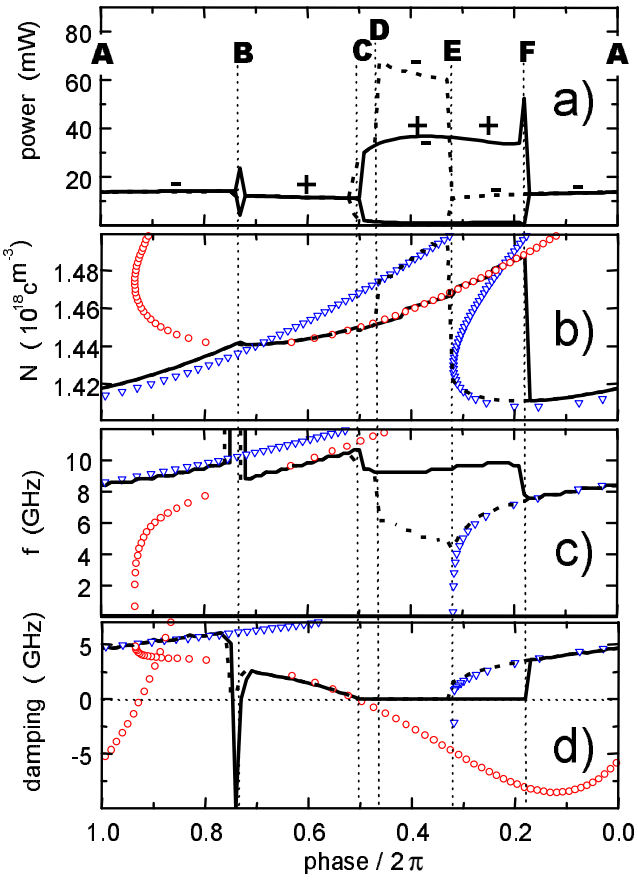

Figure 9. *Role of phase tuning.*

a) Output power calculated with the numerical time domain simulation. The phase angle φ decreases from left to right because this corresponds to increasing the phase tuning current in the experiment. It was changed in the calculations stepwise from 0 to 2π and back using the final state of Ψ and N from the previous step as initial state of Ψ and N for the next step. Dashed: increasing φ from 0 to 2π. Solid: decreasing φ back from 2π to 0. In case of SP, the maximum and minimum power during one period are given. The signs + and − at the curves indicate whether the emission wavelength belongs to the long or to the short wavelength side of the stop band of the laser section, respectively.

b) Carrier density in the laser section. Some mean carrier density during one period is drawn when the simulation yielded SP. Open circles and triangles: threshold densities of the modes on the long wave side and on the short wave side of the stop band of the laser section, respectively.

c), d) Small signal frequencies and damping constants. The symbols represent the small signal values corresponding to Eq. (8) belonging to the stationary states of the same modes as in part b). In the time domain simulation, these quantities have been determined for the stationary states by analyzing the response to small perturbations. In the SP regimes, f is the SP frequency determined from the power spectrum and the damping has been set to zero.

above the lines marks whether the long wave mode or the short wave mode of the DFB laser is lasing, respectively. To analyze the time domain data, we have independently calculated the individual threshold densities of the different modes as well as their small signal resonance frequencies $f = \omega/2\pi$ and damping constants γ corresponding to Eq. (8) and plotted as open symbols.

Several features agree with the predictions of the single mode analysis of the preceeding chapter.

- Three different types of behaviour are observed as already in Fig. 6:
  I) a stationary solution independent of the direction of phase change (between A to C and F to A),
  III) self-pulsations only (C to E), and
  II) the coexistence of a stationary and a self-pulsating solution (E to F).
- In the stationary states, the threshold density and the small signal parameters (8) agree very well with the time domain data. It is the mode with the lowest threshold density that lases in these states.
- Both the resonance frequency and the damping are considerably influenced by the dispersive reflector and can be tuned by the phase shift.
- The '+' mode exhibits a wide region of negative damping with finite f that ranges from the phase $\varphi/2\pi \approx 0.5$ (point C) down to $\varphi/2\pi \approx -0.1$ (equivalent to $\varphi/2\pi \approx 0.9$) and corresponds to region III of stable self-pulsations in Fig. 6 of the single mode analysis. In contrast, the '−' mode does not show this feature. This result is consistent with the spectral situation of Fig. 8, where only the '+' mode is on the negative slope of the reflector spectrum (criterion a) of DQS).

- Point C is a Hopf bifurcation point of the lasing '+' mode because the damping goes through zero at a finite f. Accordingly, the time domain simulation exhibits a transition from a stationary state to a self-pulsation. Our analysis shows, that this Hopf bifurcation is supercritical and corresponds to line $P_1 - P_2$ in Fig. 6.
- The frequency of the self-pulsation is smaller than the small signal resonance frequency of the corresponding stationary mode.
- For decreasing phase the self-pulsations end abruptly (point F) and show hysteresis.

There are, however, also modifications and new features not obtained within the single mode approximation.

- In point B two modes of opposite sides of the stop band coexist. We observe beating oscillations with a huge frequency corresponding to the frequency difference between the modes. However, it is not clear yet whether this phenomenon is stable.
- The SP of the long wave mode is terminated in point F by a jump into the stable '–' mode before its instability region (III in Fig. 6) is finished. This limitation of the range of self-pulsations by the presence of the '–' mode is undesirable for the application of the device as optical clock.
- Between E and F, a self-pulsating state of the '+' mode coexists with a stationary state of the '–' mode. In Fig. 6 of the single mode model, the coexisting states in region II belong to the same mode.
- The transition in E from a stationary state to a self-pulsation is connected with a saddle node bifurcation. When approaching this point from the right, a stable stationary '–' mode is lasing. Beyond E this mode disappears. This is a strong perturbation for the laser. Surprisingly, the lasing jumps into a self-pulsating short wave state although there exists a state with a much lower threshold density on the opposite side of the stop band. The nature of this transition and of the SP of the '–' mode between E and D is still under investigation.
- It should be emphasized that each of the coexisting states between D and F is stable, i.e., we have never observed in our simulations a spontaneous transition from one of these states into the other one. The sensitivity with respect to finite perturbations has however not been explored, yet.

Although being very interesting from a theoretical point of view, the participation of two modes from opposite sides of the stop band is less useful for the application of the devices in the optical communication. It reduces the phase range available for the wanted DQS self-pulsations of the '+' mode. The hysteresis requires to follow carefully a certain path to the desired point of operation. Therefore we are looking for a design of the dispersive reflector that suppresses the influence of the competing modes.

4.2. Grating detuning as design parameter

For this purpose we have used the static detuning δ between the two DFB gratings (cf. Fig. 1) as a new design parameter. This was motivated by the observation that the nonpulsating '–' mode in Fig. 8 gets a larger feedback from the reflector section than the pulsating '+' mode. It can be expected that the region of self-pulsations is enhanced when the feedback of the nonpulsating mode is diminished by, e.g., an appropriate detuning.

To check this hypothesis, the detuning parameter δ has been varied over a 15 nm wide range with steps of 0.1 nm keeping the laser configuration and all parameters as in the previous subsection. For every δ, the phase angle φ was tuned downwards from 2π down to 0 in 50 equidistant steps. The SP-regions obtained are drawn in the upper part of Fig. 10 as islands with thick black borders. Island 1 in the center belongs to the spectral correlation of Fig. 8 and can be addressed by the thermal λ-shift in the present generation of devices.[6] Note, that the SP on the '+' mode discussed in the previous chapter are contained in this island.

For larger detunings, several new SP islands appear (note that islands touching the border $\varphi = 2\pi$ continue at $\varphi = 0$ and vice versa, due to the phase periodicity). The reflectivity spectra drawn in the lower part of Fig. 10 for the islands 2 to 5 show that they belong to other possible combinations of one of the two potentially lasing modes with a negative slope of one of the different lobes of the reflector spectrum. One can see, that in some cases the feedback from reflector section for the competing DFB mode is smaller. Therefore, in these cases we can expect smaller sensitivity of the device to these modes and partially avoid the mode hops.

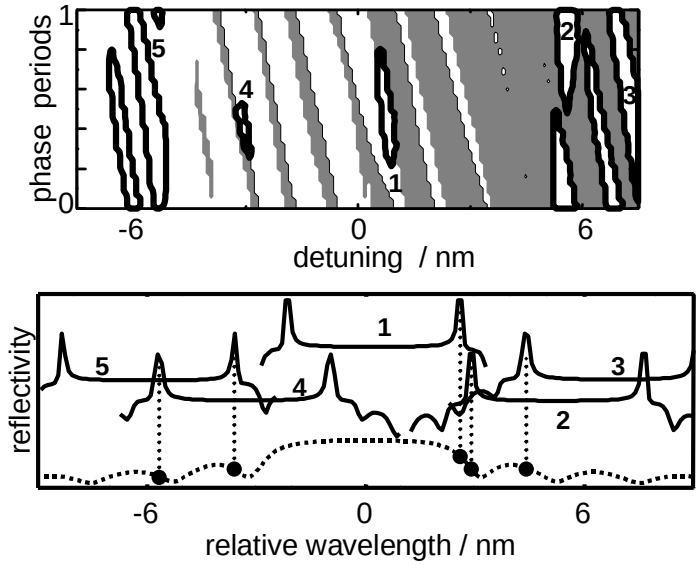

Figure 10. *Upper part: different areas of SP in detuning/phase plane (thick lines). Grey background indicate that short mode is lasing. White background shows that long mode is lasing. Lower part: calculated feedback spectra of the reflector section (dotted) and different positions of the feedback spectra of gain section (solid) for different values of detuning. The dashed straight lines indicate the lasing mode in each situation. The numbers indicate correspondence between SP islands and spectral correlation.*

Being larger and less sensitive to mode jumps, these new islands are improved compared to island 1. The existence of such islands has been also verified experimentally using first devices with detuned gratings.[15]

It is worth to note, that even having very small feedback for competing DFB mode, the changes of phase can cause the jump to this mode from the more strongly feeded mode. These jumps are indicated in the upper part of Fig. 10, where for the not very big detuning values we can see an exchange of white and grey backgroud areas. Nevertheless, these mode jumps disappeared totally for large detunings, where the new SP areas were detected. As expected, this suppression of the nonpulsating mode leaded to noticeable larger pulsation regions compared to region 1.

5. CONCLUSION

It has been demonstrated theoretically that the dynamical behaviour of a DFB laser can be goal-directed modified by means of an integrated passive dispersive reflectors (PDR). We started with a comprehensive analysis of the single mode case. In this frame it was shown that the resonance of the axial excess factor of spontaneous emission K_z caused by the PDR plays the crucial role. It can be used either for achieving fast switching by suppressing relaxation oscillations or for generating self-sustained pulsations by undamping these oscillations. A typical bifurcation diagram was constructed showing regions with either stable stationary states, or stable self-pulsations, or the coexistence of stable stationary and stable self-pulsating states (hysteresis). A full time-domain simulation taking into account all relevant modes and using the phase shift as experimentally accessable bifurcation parameter confirmed these results but exhibited also new features. The laser emission was essentially single mode, however not always in the same mode but either in a long wave mode or in a short wave mode. This presence of a second mode complicated the bifurcation scenario and reduced the parameter region available for the application of the self-pulsations. The latter effect can be avoided by using devices with appropriately detuned gratings.

ACKNOWLEDGMENTS

Parts of this work have been supported by Deutsche Forschungsgemeinschaft (DFG). One of the authors (U.B.) wants to acknowledge the DFG for partially supporting the conference expanses. V.Tronciu acknowledges financial support from Alexander von Humboldt Foundation and from Weierstrass Institut Berlin.

REFERENCES

1. J. Sacher, D. Baums, P. Panknin, W. Elsässer, and E. O. Göbel, "Intensity instabilities of semiconductor lasers under current modulation, external light injection, and delayed feedback," *Phys. Rev. A* **45**, pp. 1893–1905, 1992.

2. K. Petermann, "External optical feedback phenomena in semiconductor lasers," *IEEE J. of Selected Topics in Quantum Electronics* **1**, pp. 480–489, 1995.
3. M. Yousefi and D. Lenstra, "Dynamical behaviour of a semiconductor laser with filtered external optical feedback," *IEEE J. Quantum Electron.* **35**, pp. 970–976, 1999.
4. B. Sartorius, M. Möhrle, S. Reichenbacher, and W. Ebert, "Controllable self-pulsations in multisection DFB lasers with an integrated phase-tuning section," *IEEE Photon. Technol. Lett.* **7**, pp. 1261–1263, 1995.
5. B. Sartorius, C. Bornholdt, O. Brox, H. Ehrke, D. Hoffmann, R. Ludwig, and M. Möhrle, "All-optical clock recovery module based on a self-pulsating DFB laser," *Electron. Lett.* **34**, pp. 1664–1665, 1998.
6. B. Sartorius, M. Möhrle, S. Reichenbacher, H. Preier, H.-J. Wünsche, and U. Bandelow, "Dispersive self-Q-switching in self-pulsating DFB lasers," *IEEE J. Quantum Electron.* **33**, pp. 211–218, 1997.
7. H. Wenzel, U. Bandelow, H. J. Wünsche, and J. Rehberg, "Mechanisms of fast self pulsations in two-section DFB lasers," *IEEE J. Quantum Electron.* **32**(1), 1996.
8. U. Bandelow, R. Schatz, and H.-J. Wünsche, "A correct single mode photon rate equation for multisection lasers," *IEEE Photon. Technol. Lett.* **8**(5), pp. 614–617, 1996.
9. U. Bandelow, H. J. Wünsche, B. Sartorius, and M. Möhrle, "Dispersive self-Q-switching in DFB lasers – theory versus experiment," *IEEE J. of Selected Topics in Quantum Electronics* **3**(2), pp. 270–278, 1997.
10. V. Tronciu, H.-J. Wünsche, J. Sieber, K. Schneider, and F. Henneberger, "On the dynamics of single mode lasers with passive dispersive reflector." Preprint No. 541, WIAS – Berlin, 1999.
11. U. Bandelow, H.-J. Wünsche, and H. Wenzel, "Theory of self-pulsations in two-section DFB lasers," *IEEE Photon. Technol. Lett.* **5**, pp. 1176–1179, 1993.
12. O. Kjebon, R. Schatz, S. Lourdudoss, S. Nilsson, B. Stålnacke, and L. Bäckbom, "30 GHz direct modulation bandwidth in detuned loaded InGaAsP DBR-lasers at 1.55 μm wavelength," *Electron. Lett.* **33**(6), pp. 488–489, 1997.
13. E. J. Doedel, A. R. Champneys, T. F. Fairgrieve, Y. A. Kuznetsov, B. Sandstede, and X. Wang, "**Auto 97** continuation and bifurcation software for ordinary differential equations," March 1998.
14. M. Radziunas, H.-J. Wünsche, B. Sartorius, O. Brox, D. Hoffmann, and K. Schneider, "Modeling of self-pulsating DFB lasers." Preprint No. 516, WIAS – Berlin, 1999.
15. M. Radziunas, H.-J. Wünsche, B. Sartorius, H.-P. Nolting, K. Schneider, O. Brox, and D. Hoffmann, "Modeling of new grating designs for self-pulsating DFB lasers," in *Integrated Photonics Research, OSA Technical Digest*, pp. 358–360, Optical Society of America, (Washington DC), 1999.